Enhanced μ Rhythm Extraction Using Blind Source Separation and Wavelet Transform

Siew-Cheok Ng* and Paramesran Raveendran, *Senior Member, IEEE*

***Abstract*—The μ rhythm is an electroencephalogram (EEG) signal located at the central region of the brain that is frequently used for studies concerning motor activity. Quite often, the EEG data are contaminated with artifacts and the application of blind source separation (BSS) alone is insufficient to extract the μ rhythm component. We present a new two-stage approach to extract the μ rhythm component. The first stage uses second-order blind identification (SOBI) with stationary wavelet transform (SWT) to automatically remove the artifacts. In the second stage, SOBI is applied again to find the μ rhythm component. Our method is first compared with independent component analysis with discrete wavelet transform (ICA-DWT) as well as SOBI-DWT, ICA-SWT, and regression method for artifact removal using simulated EEG data. The results showed that the regression method is more effective in removing electrooculogram (EOG) artifacts, while SOBI-SWT is more effective in removing electromyogram (EMG) artifacts as compared to the other artifact removal methods. Then, all the methods are compared with the direct application of SOBI in extracting μ rhythm components on simulated and actual EEG data from ten subjects. The results showed that the proposed method of SOBI-SWT artifact removal enhances the extraction of the μ rhythm component.**

***Index Terms*—μ rhythm, artifact removal, blind source separation (BSS), second-order blind identification with stationary wavelet transform (SOBI-SWT).**

I. Introduction

THE μ rhythm is extensively used in the study of changes in the brain during motor activity. Basic research to understand the changes in the μ rhythm due to hand movement with varying load [1], repetitive hand movement [2], switching of hand task [3], motor imagery [4], and the differences in hand and foot μ rhythm [5] have been carried out. Apart from this, the effects of aging [6] and gravity [7] on the μ rhythm have also been studied. The μ rhythm has been found to be an indicator of various medical conditions such as autism [8], Down syndrome [9], and Parkinson's disease [10]. Neurofeedback based on the μ rhythm was shown to be effective in changing the electroencephalogram (EEG) and behavior of autistic children [11]. The brain–computer interface, which attempts to decipher the intention of a person using the changes in the μ rhythm, has been actively researched [12], [13].

Manuscript received November 24, 2008; revised February 10, 2009 and April 18, 2009. First published May 19, 2009; current version published July 15, 2009. This work was supported by the University of Malaya under Research Grant SF037/2007A. *Asterisk indicates corresponding author.*

*S.-C. Ng is with the Department of Biomedical Engineering, University of Malaya, 50603 Kuala Lumpur, Malaysia (e-mail: siewcng@um.edu.my).

P. Raveendran is with the Department of Electrical Engineering, University of Malaya, 50603 Kuala Lumpur, Malaysia (e-mail: ravee@um.edu.my).

Color versions of one or more of the figures in this paper are available online at http://ieeexplore.ieee.org.

Digital Object Identifier 10.1109/TBME.2009.2021987

A historical review [14] stated that an earlier research found the μ rhythm in about 10% of the human population. Later on, with the development of digital signal processing methods, the μ rhythm was shown in almost all the subjects [15]. A bandpass filter is applied onto the EEG signal from the motor cortex region based on the μ rhythm frequency band. However, the μ rhythm being in the range of microvolts is highly susceptible to artifacts.

The removal of artifacts has generated immense interest in EEG research. There are three main methods of having clean EEG data. The first method is to ignore all segments of EEG that contain artifacts and process only the segments that are clean [6]–[8]. However, such a method may remove most of the EEG of interest and may not leave enough data for analysis. The second method requires the subject to be actively aware of not producing any artifacts. However, this may change the EEG activity [16]. Thus, the third method, which is to remove the artifact component while maintaining the EEG component for the segment of EEG that contains artifacts, has been actively developed [17]–[31].

In the third method, the two main techniques that are used to remove the artifacts are using filters and finding the artifact component that is to be removed. The assumption that the artifact and the EEG have different frequency components allows filters to remove artifacts in the frequency domain. The filtering methods that have been used include linear filters [17], adaptive filters [18], and wavelets [19]. The discrete wavelet transform (DWT) algorithm is frequently used for artifact removal [19], [20]. However, the stationary wavelet transform (SWT) algorithm has been used to remove electrooculogram (EOG) artifacts [21], as it provides good temporal resolution. Brychta *et al.* [32], [33] compared SWT with DWT for spike detection and found SWT to be better due to its translation invariant property. Since electromyogram (EMG) artifacts are rather spiky in nature, SWT may be a better alternative than DWT in EMG artifact removal.

As for the second technique, there are various ways of finding the artifact component such as placing electrodes near the source of the artifacts or using a component separation method based on blind source separation (BSS). This technique finds the effect of the artifact signals on to each electrode. Then, the artifacts are subtracted based on the weights from those electrodes. There are two types of BSSs that are based on the second-order statistics (SOS) and higher-order statistics (HOS). The independent component analysis (ICA) is based on HOS. The extended infomax ICA and fastICA algorithms have been applied to remove artifacts such as EOG [22], EMG [23], [24], and ECG [25]. However, both the ICA algorithms require random initialization

and iterative computation to obtain the final estimated source. On the other hand, the SOS does not have these drawbacks but assumes the data to be temporally correlated. One of the popular SOS algorithms, the second-order blind identification (SOBI), has been used to separate the EEG signal into independent sources for further processing [26], as well as for EOG and EMG artifacts removal [27]. Comparative studies have shown that SOBI performs better than ICA for removing the EOG artifact [28]. Furthermore, the SOBI algorithm has faster processing time and requires less training samples [28].

However, both techniques have certain distinct drawbacks. It is generally assumed that the EOG artifacts are within the δ frequency band (0–4 Hz) while the EMG artifact is within the β frequency band (>13 Hz) [34]. Thus, these artifacts would not contribute to the μ rhythm component that falls in the α frequency band (8–12 Hz). However, studies have shown that EOG frequency extends to 54 Hz [35] and EMG frequency exists at 8 Hz onward [36]. This may indicate that filtering based on frequency on its own may create inaccurate results. BSSs assumed that the artifacts can be localized into a few components to be eliminated [31]. However, later studies have shown that the artifact components may have some EEG signals [37]. Thus, when the whole artifact component is removed, some EEG signals will also be removed.

Recently, the wavelet-ICA (WICA) for EEG artifact removal using the ICA-DWT algorithm was proposed by Castellanos and Makarov [29] and Inuso *et al.* [30]. However, it should be noted that the idea of WICA was proposed way back in 2004 [38] to remove ECG and pulse artifacts from surface EMG signals. Generally, WICA localizes the artifacts into a few components, where the artifact removal method will be applied on to it. The advantage here is that the other components are not distorted due to the artifact removal process as it is applied only on those components that contain artifacts. Furthermore, it has been shown that the WICA method does not artificially enhance the coherence between the different EEG channels as in the direct application of the ICA method for artifact removal [29].

After removing the artifacts, obtaining the μ rhythm may seem quite straightforward by using the bandpass filter [5]. However, this method requires the information about the optimal location and frequency of the μ rhythm specific for each subject [39]. Furthermore, if the α rhythm has the same frequency as the μ rhythm, this method may not be able to separate them. The μ rhythm component obtained from this method would only show its strength at the optimal location. In order to analyze the relation between both hemispheres, further analysis using the coherence method is required. The inadequacy of this method has actually led to the introduction of BSS to the extraction of EEG signals [31].

Given the strengths and inadequacies of the aforementioned methods, it seems logical to ask, "Can we get better results if we combine them into a two-stage approach that will enhance the extraction of the μ rhythm?"

We proposed a two-stage method where the BSS method is applied not once but twice for the extraction of the μ rhythm. The first stage involves removal of artifacts, while the second stage extracts the μ rhythm component. From the review, it has been shown that for artifact removal, SOBI performs better than ICA [28] and SWT is better at detecting spikes than DWT [33]. Based on this, we postulate that the SOBI-SWT algorithm should perform better than the ICA-DWT algorithm for the removal of artifacts. Thus, for the first stage, we use the SOBI-SWT algorithm for artifact removal and SOBI again for the extraction of the μ rhythm in the second stage. A set of simulated data is used to compare the performance of SOBI-SWT with the ICA-DWT as well as their combinations (SOBI-DWT and ICA-SWT) in the removal of artifacts. Then, the two-stage approach would be compared with the direct application of SOBI to extract the μ rhythm from simulated data as well as actual EEG data.

This paper is organized as follows. Section II deals with wavelet transform and BSS signal processing methods. A detailed description of the simulated signal and the signal processing methods will be presented in Section III. In Section IV, the experimental results of removal of artifacts will be shown and discussed. This is then followed by the experimental results for extraction of the μ rhythm in Section V. The conclusion and future work in Section VI concludes the study.

II. Signal Processing Methods

The mathematics and algorithm involved in this paper will be presented in this section. The wavelet transform and BSS are the main algorithms involved and will be discussed separately in Section II-A and II-B. The new proposed method, which involves two stages of processing to enable better extraction of relevant independent components, will then be presented.

A. Wavelet Transform

The wavelet transform is an efficient method of filtering a signal into different frequency bands. The signal with n samples, $x(t) = \{x(1), \ldots, x(n)\}$, is decomposed using a low-pass filter using a wavelet function $\phi(t)$ to extract the approximation signal $A(t)$ and a high-pass filter using the scaling function $\psi(t)$ to extract the detail signal $D(t)$. Only the approximation signal $A(t)$ is used for the next level of decomposition. The wavelet decomposition into approximation and detail signal are defined as follows:

$$A_i(t) = \sum_{k=-\infty}^{\infty} A_{i-1}(k)\phi_i(t-k) \tag{1}$$

$$D_i(t) = \sum_{k=-\infty}^{\infty} A_{i-1}(k)\psi_i(t-k). \tag{2}$$

The reconstruction of the wavelet coefficient is defined as

$$x(t) = \sum_{k=-\infty}^{\infty} A_L(k)\phi_i'(t-k) + \sum_{i=1}^{L}\sum_{k=-\infty}^{\infty} D_{i+1}(k)\psi_i'(t-k). \tag{3}$$

For DWT, the values of $A_i(t)$ are downsampled by removing alternate values for the next level. However, for SWT, the values of $\phi_i(t)$ and $\psi_i(t)$ are upsampled by padding zeros between all the values for the next level.

B. Blind Source Separation

A review on BSS [40] states that it was introduced in the mid-1980s to obtain the individual source signals for a biological problem from the available mixed multidimensional data. Basically, the BSS problem can be formulated as

$$X(t) = A\,S(t) \tag{4}$$

where $X(t) = \{x_1(t), \ldots, x_{nx}(t)\}$ is the time series data from nx recorded channels, $S(t) = \{s_1(t), \ldots, s_{ns}(t)\}$ is the unknown ns sources, and A is an unknown $nx \times ns$ constant mixing matrix. Thus, the BSS problem is to find the values for the mixing matrix A and the source signals $S(t)$. It should be noted that if either A or $S(t)$ is known, finding the other value would be trivial. In most cases, it is assumed that the number of recorded channels nx is equal to the number of sources ns.

The ICA algorithm that is applied in this paper is the fastICA, as it can produce the results faster. The fastICA maximizes the non-Gaussianity using the negentropy method. The negentropy is estimated using

$$J(y) \propto [E\{G(y)\} - \{G(\nu)\}]^2 \tag{5}$$

where $J(y)$ is the negentropy of y, $E\{\cdot\}$ denotes the expected value, ν is a Gaussian random variable of zero mean and unit variance, and G is the contrast function, $\log(\cosh(\cdot))$. The algorithm to compute the fastICA using the negentropy method is given by Hyvarinen *et al.* [41].

The SOBI algorithm was first introduced by Belouchrani *et al.* [42]. A more robust algorithm was introduced by Belouchrani and Cichocki [43] to solve the problem of using a time lag close to zero and the requirement of the white noise assumption. The SOBI algorithm attempts to perform the joint approximate diagonalization on to the set of time-lagged covariance matrix obtained by

$$\hat{R}(p_i) = \frac{1}{N} \sum \overline{X}(t)\overline{X}^T(t - p_i). \tag{6}$$

The complete algorithm to compute robust SOBI is given by Cichocki and Amari [44].

C. Proposed Method

A two-stage method to extract the μ rhythm will be discussed in this section. The first stage automatically removes artifacts while the second stage extracts the μ rhythm components. In the first stage, BSS is used in conjunction with the wavelet method to remove the artifacts [29]. This approach has an advantage over using only either wavelet or BSS method to remove artifacts. Artifact removal using the wavelet method is based on the assumption that if there is an outlier in a certain frequency decomposition, it implies that the outlier is an artifact. There are two problems with this assumption. The first is if the amplitude is less than the signal, then the wavelet method would not be able to remove that artifact. The second is when the artifact is removed, it may remove some EEG components at the same time segment and frequency range where it removed the artifact.

The BSS method of artifact removal, on the other hand, assumes that the artifacts can be isolated into a single component. This may be true if there are special channels dedicated to collect all the individual artifacts. There may be extra channels to obtain the data for EOG artifacts but there are no extra channels to obtain data for EMG artifacts. Studies have shown that there is usually some residue of EEG in the BSS component that contains artifacts [37]. Furthermore, using the BSS method to remove artifacts also removes one of the components and thus making the mixture an underdetermined problem. At the same time, it also artificially enhances the coherence between all the electrode channels [29].

Thus, the usage of BSS to decompose the signal into independent components and then applying wavelet for artifact removal on the components has the following advantages.

1) *Less distortion to the EEG:* Since the artifacts are grouped into a few components, the removal of artifacts using the wavelet method is only applied on to these components and leaves the other components as they are.
2) *Increases the amount of artifacts removed:* When the artifacts are grouped into a few components, their relative amplitude would be very much larger than the EEG signal and thus allows better detection and removal of artifacts.
3) *Allows redecomposition of the processed EEG signal:* The EEG signals in the artifact dominant components are maintained; thus, this allows the artifact removed signal to be redecomposed to find the EEG source of interest.

The wavelet function used in the current study is the fourth-order Daubechies (db4), which has been frequently applied in other EEG studies [30], [38], [45]. The level-dependent fixed-form threshold of the detail signal $D(t)$ for all the levels as well as the analyzing signal $A(t)$ for the highest decomposition level is found using (7). The signal for each decomposition level is compared with their corresponding threshold to find the artifacts. The segment of the signal that is more than the threshold is considered as artifact and is removed by replacing those values with zeros. The fixed form threshold [29], [32], [33] is given by (7) as shown in the following:

$$K_i = \sqrt{2\log(N_i)}\,\sigma_i \tag{7}$$

where N_i is the number of sample in that level and $\sigma_i = \text{median}(D_i(t))/0.6745$. For the highest level of analyzing signal, $A_i(t)$ replaces $D_i(t)$ in the computation of σ_i.

For the first stage, our proposed method uses SOBI-SWT to remove the artifacts. This combination is proposed due to the increase in performance when SOBI is compared with ICA [28] and also SWT as compared to DWT [32]. It must be noted that SOBI and SWT were used independently in the comparative studies [28], [32]. In this paper, both methods are applied hand in hand similar to the approach of Castellanos and Makarov [29].

As for the second stage, the SOBI algorithm is used for the redecomposition. This is because, the computation is faster and produces the same results as long as the time-lagged covariance used is the same. Furthermore, a smaller component number would be indicative of a more dominant component as SOBI sorts out the components from the most dominant to the least dominant.

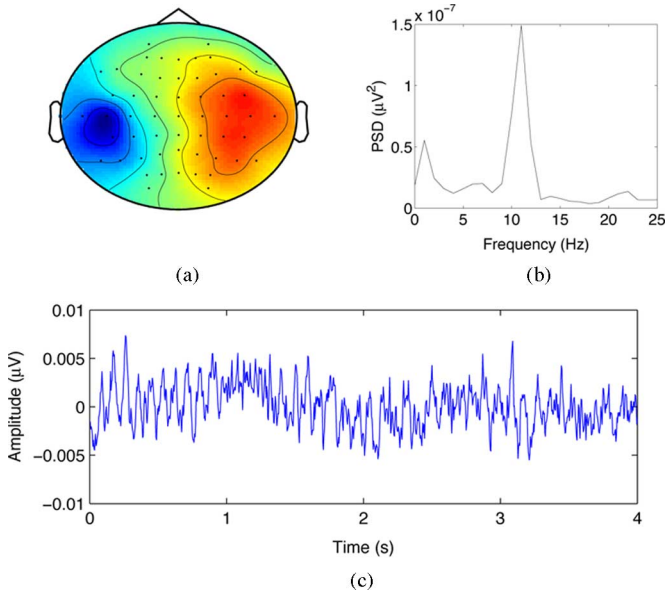

Fig. 1. Extraction of the μ rhythm. (a) Topographical. (b) Frequency analysis. (c) μ rhythm component.

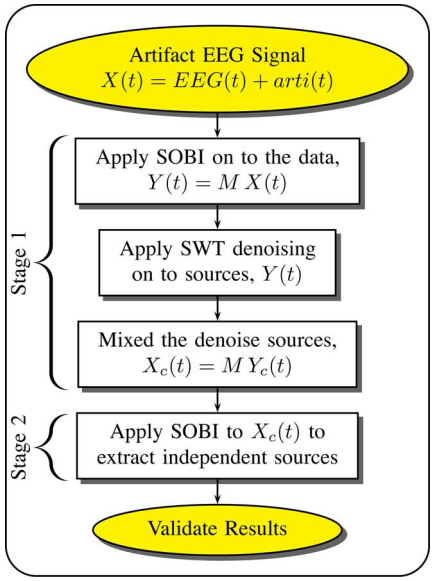

Fig. 2. BSS-wavelet algorithm to enhanced independent components.

Generally, the μ rhythm component is determined by checking the topographical plot and the dominant frequency in the α frequency band. A typical example of the technique used to determine the μ rhythm component is shown in Fig. 1. First, we have to determine whether a certain component has strong activities emanating from the motor cortex region [refer Fig. 1(a)]. Then, a spectral analysis done on that component would indicate a peak at the μ rhythm frequency as shown in Fig. 1(b). Finally, we checked whether there is any artifact component which is stronger than the μ rhythm in the time domain [refer Fig. 1(c)] based on the signals that are morphologically similar to the EOG or EMG artifacts.

The algorithm for this two-stage approach is shown in Fig. 2.

III. EEG Data Set

In this study, we used two different sets of data. The first set is the actual EEG data from ten subjects that contain artifacts. The second set is a simulated set of EEG data obtained by processing the data from three of the ten subjects. The methods of obtaining these two sets of data are discussed below.

A. Actual EEG Data

The EEG data are recorded from ten healthy male subjects. A 64-channel electrocap is placed on the subject. However, only 55 EEG channel recordings are collected as the other channels are used to collect EOG and EMG signals. It should be noted that only the 55 EEG channel recordings are used for the processing. The EOG recordings are just to reconfirm the existence of EOG artifacts. The EMG recordings are obtained from the arm muscles to indicate their level of activity during the experimental task. The signals are sampled at 256 Hz.

This experimental protocol was carried out to study the effects of fatigue on the brain signal, particularly the μ rhythm at the motor cortex region. When the experiment begins, the subject is required to close his eyes for 2 min and then to keep his eyes open for the next 2 min. This is repeated two times before and after the experimental task. The experimental task requires the subject to grip a dynamometer as hard as possible for 30 s with the right hand. This is followed by a 15 s break. Then the left hand will grip the dynamometer for another 30 s followed by another 15 s break. This task is repeated for 30 times or until the subject could no longer continue with the task. Artifacts such as EOG and EMG can be observed from the EEG data although the subject has been instructed not to create artifacts. The four sets of EEG signals during the eyes-closed condition (2 min) are joined together to form a set of EEG data that is 8 min in duration. The same is applied for the eyes-opened condition. These sets of data are used for processing.

B. Simulated EEG Data

For the simulated data, the raw EEG data are obtained from three subjects. Only 19 channels corresponding to the International 10–20 system are used. This is because if 55 channels are used, a 5 min segment of data would be required for the ICA algorithm to learn. Furthermore, it would be more challenging to remove the same number of artifact sources from 19 channels as compared to 55 channels. This is because, the number of dominant EEG signal source that is observable is only about 5–15 [46].

Two types of data are then generated from the original data set. The first type is considered reference EEG while the second type consists of reference artifacts such as EOG and EMG. There are eight individual artifact components: two from EOG and six from EMG. Based on this eight individual artifact components, we obtained four combinations: EOG (VEOG + HEOG), EMG_{rail} ($\text{EMG}_{\text{rail1}} + \text{EMG}_{\text{rail2}} + \text{EMG}_{\text{rail3}}$), $\text{EMG}_{\text{noise}}$ ($\text{EMG}_{\text{noise1}} + \text{EMG}_{\text{noise2}} + \text{EMG}_{\text{noise3}}$), and EOGnEMG ($\text{EOG} + \text{EMG}_{\text{rail}} + \text{EMG}_{\text{noise}}$). For each of the twelve types of artifacts, they are mixed into the reference EEG signal based

on different SNR. The SNR that are considered is from −50 to 50 dB. From 10 to 50 dB (as well as −10 to −50 dB), the step of 10 dB is used while from −10 to 10 dB, the step of 1 dB is used.

1) Reference EEG: The reference EEG is obtained from 60 s of EEG data during the eyes-closed condition. For the eyes-closed condition, the visual α rhythm is rather dominant and is useful to determine whether the μ rhythm is able to be extracted even in the presence of stronger signals in about the same frequency band. For a more representative study, another set of reference EEG is obtained from the eyes-opened condition for comparison. However, the subject may still generate some weak EMG and EOG artifacts. First, the EEG data are visually checked to identify any obvious EMG or EOG artifacts. The artifacts are then removed using wavelet denoising to give us the reference EEG data.

2) Reference Artifact (EOG): There are two types of EOG artifacts: vertical EOG (VEOG) and horizontal EOG (HEOG). The EOG artifacts are obtained by applying SOBI on to the segment of EEG data that has obvious eye movements. Based on the obtained topographical map, it is easy to identify which source represents VEOG and HEOG. Then, that source would be extracted and segments of data that obviously does not contain EOG would be eliminated or replaced with zeros. The effects of the EOG on to each channel would be obtained by multiplying the processed source with the topographical map weights.

3) Reference Artifact (EMG): There are three types of EMG artifacts [36] with distinctive patterns: a) noise-like, b) railroad cross-tie, c) β rhythm-like. In the current study, only the noise-like and railroad cross-tie EMG artifacts are considered as the β rhythm-like EMG can only be determined from controlled experiment. Furthermore, many more subjects indicated the presence of noise-like and railroad cross-tie EMG artifacts as compared to the β rhythm-like EMG [36]. Similar methods as reference artifact (EOG) extraction are used to obtain the EMG artifacts. The EMG artifacts are usually generated from more than one muscle and from the left and right regions of the scalp. Thus, three different sources generated from different topographical locations for noise-like and railroad cross-tie are used in this study.

IV. Experimental Study on Removal of Artifacts

In this section, the performance of SOBI-SWT is compared to ICA-DWT, SOBI-DWT, ICA-SWT, and regression method for artifact removal. Fig. 3 shows the typical signals that existed in the various stages of processing. For clarity, the signal segment of only 3 s are shown for five of the 19 channels available. The scale of the y-axis is the same for all the channels.

The *ReferenceEEG* and *ReferenceArtifact* are both simulated signals. The μ rhythm can be seen at the C3 location from Fig. 3(a) as the eyes-opened condition data are used here. For the eyes-closed condition, the μ rhythm at the C3 location may be obscured by the visual α rhythm. The *ReferenceArtifact* shown in Fig. 3(b) is the EMG noise-like type. It can be seen that the artifact is strongest at the temporal regions. The *ReferenceArtifact* is added to the *ReferenceEEG* to obtain *EEG + Artifact*.

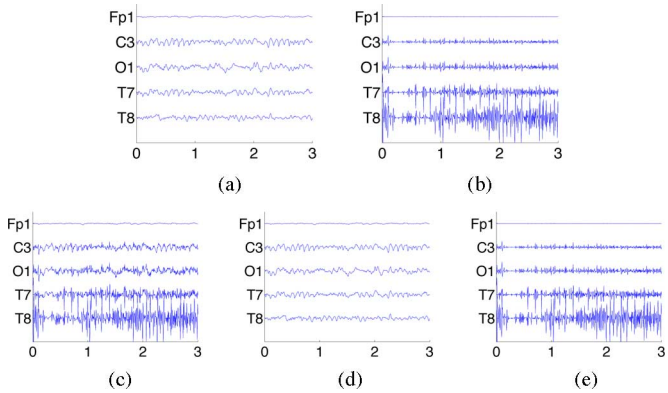

Fig. 3. Sample of EEG and artifact before, during, and after artifact removal. (a) *ReferenceEEG*. (b) *ReferenceArtifact*. (c) *EEG + Artifact*. (d) *ProcessedEEG*. (e) *RemovedArtifact*.

The *EEG + Artifact* is the raw data that is processed using the artifact removal algorithms stated earlier. It can be seen from Fig. 3(c) that the μ rhythm at the C3 location is contaminated with the EMG artifacts. After processing, we would obtain the *RemovedArtifact* and *ProcessedEEG* signal. From Fig. 3(d), the μ rhythm for the *ProcessedEEG* at the C3 location is again clearly seen.

Ideally, the *ProcessedEEG* should be exactly the same as the *ReferenceEEG* while the *RemovedArtifact* should be exactly the same as the *ReferenceArtifact*. Visually, the *RemovedArtifact* and *ProcessedEEG* seem to be very similar to the original ones. Thus, two methods which are the correlation coefficient and the relative root mean squared error (RRMSE) are used to quantify the performance of the artifact removal methods. The performance of a certain artifact removal algorithm is based on two factors, which are the ability to remove the artifact and to maintain the EEG signal as much as possible.

A. Correlation Coefficient

In this section, the performance of the five methods for artifact removal is quantified using the correlation coefficient method. For the EOG artifacts, all the five methods are applied. However, for the EMG artifacts, only the four BSS-wavelet methods are applied as there are no reference artifact for regression algorithm to be applied.

For the application of the regression method, two reference EOG signals (HEOG and VEOG) are obtained by mixing the frontal EEG (Fp1 and Fp2) into the corresponding *ReferenceArtifact*. The Bayesian Adaptive Regression Splines (BARS) algorithm is used to remove the EEG signals from the reference EOG signals before the regression algorithm is applied [37], [47]. The BARS program is obtained from http://lib.stat.cmu.edu/kass/bars/bars.html.

The two main factors to assess the performance of the artifact removal methods are shown in Fig. 4 for one subject during the eyes-closed condition. For Fig. 4(a)–(d), a bigger correlation coefficient value shows that more artifact components have been removed. As for Fig. 4(e)–(h), a bigger correlation coefficient

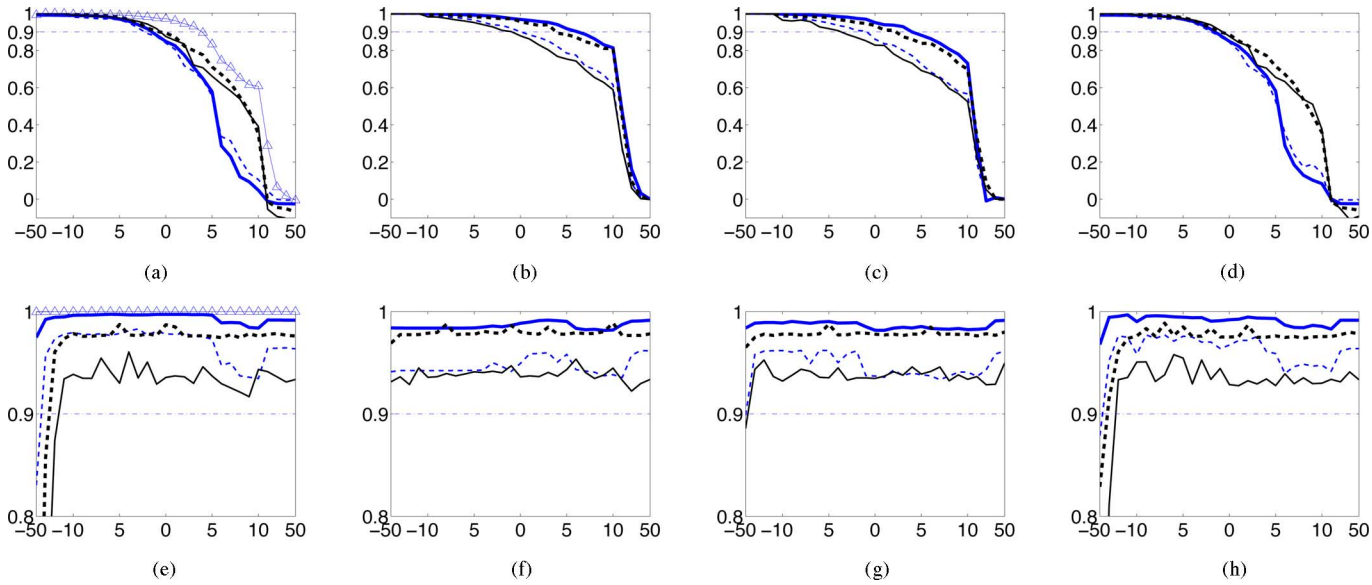

Fig. 4. Comparison between the performance of SOBI-SWT (thick continuous line), SOBI-DWT (thin broken line), ICA-SWT (thick broken line), and ICA-DWT (thin continuous line) for different artifacts. For the EOG (a and e), the regression method is the line with the triangle marker. The y-axis indicates the correlation coefficient while the x-axis is the SNR of the artifact mixture in dB. (a) EOG artifacts. (b) EMG_{rail} artifacts. (c) $\text{EMG}_{\text{noise}}$ artifacts. (d) EOGnEMG artifacts. (e) EOG signal. (f) EMG_{rail} signal. (g) $\text{EMG}_{\text{noise}}$ signal. (h) EOGnEMG signal.

value indicates less EEG signals have been inadvertently removed during the removal of the artifact.

Generally from Fig. 4(a)–(d), it can be seen that as the SNR increases, the ability of all the five algorithms to remove the artifacts is reduced. This is expected as the BSS-wavelet method for artifact removal assumes that the amplitude of the artifact is larger than the amplitude of the signal. Thus, for high SNR, the amplitude of the artifact would be less than the signal and is not removed. The BARS algorithm could not have found the spline that represents the EOG artifacts for high SNR. Thus, the reference EOG for the regression method would be inaccurate at high SNR. However, this is not a cause for concern. If the SNR is large enough, then the artifact can be ignored as its effects on the signal would be almost negligible.

A broken line at the correlation coefficient value of 0.9 can be seen from all the graphs in Fig. 4. This value of 0.9 is considered as the acceptable threshold for the performance of a certain algorithm. Fig. 4(a)–(d) would be indicative of successful artifact removal. As for Fig. 4(e)–(h), it would be indicative of an acceptable level of distortion introduced to the reference EEG signal.

As shown in Fig. 4(a), the regression method outperforms all the BSS-wavelet methods in removing EOG artifacts. However, it should be noted that the EOG usually exist for SNR < 0 dB. Thus, the performance of all the methods would be similar in the practical range of EOG. Based on Fig. 4(b)–(c), it is clear that SOBI-SWT and ICA-SWT are better at removing EMG artifacts whether they are the railroad cross-tie or the noise-like type. It is interesting that the usage of SWT instead of DWT is much better at removing EMG artifacts while the usage of SOBI instead of ICA would only improve the artifact removal slightly. Fig. 4(d) seems to produce a graph that is very similar to Fig. 4(a). This is as expected as the EOG artifacts have much larger amplitude as compared to EMG artifacts. Thus, a mixture of them would generate a result more similar to that of the EOG artifact removal performance.

Based on Fig. 4(e)–(h), although all the methods seemed to produce acceptable results for all the artifacts, SOBI-SWT produced the least distortion among all the BSS-wavelet methods. It is interesting to note that the regression method produced almost no distortion at all when removing EOG as seen from Fig. 4(e). It can be seen that ICA-DWT produced the worst distortion among all the artifact removal methods. SOBI-DWT and ICA-SWT showed similar results for EOG artifacts. However, ICA-SWT is slightly worse than SOBI-SWT while SOBI-DWT is slightly better than ICA-DWT for the EMG artifacts case. Furthermore, it seems that the changes in the SNR have no effect on the performance of SOBI-SWT. However, the other three methods seemed to remove a significant amount of EEG signals for SNR < -30 dB for the EOG artifact.

The threshold of correlation coefficient >0.9 indicates that a certain algorithm has successfully removed artifacts. Table I shows the highest possible SNR where the different algorithms could still successfully be applied. These values are the average of the three subjects for both the eyes-closed and eyes-opened conditions. It can be seen that for the eyes-opened condition, the ability to remove artifacts is better than eyes-closed condition. This is to be expected as the visual α rhythm is desynchronized in eyes-opened condition. Thus, the EEG signal would have less dominant EEG and will allow the artifacts to have larger values to be removed by the threshold method. Generally, we can see from Table I that for the removal of EMG artifacts, the SOBI-SWT method showed the best performance while the regression method performed best in removing EOG artifacts.

1) Comparative Performance of SOBI versus ICA and SWT versus DWT: It would be interesting to study whether a change

TABLE I
MEAN OF THE HIGHEST SNR FOR THE DIFFERENT ARTIFACTS THAT CAN BE SUCCESSFULLY REMOVED FOR EYES CLOSED AND OPENED (EYES OPENED IN BRACKETS)

Artifacts	Regression	SOBI-SWT	SOBI-DWT	ICA-SWT	ICA-DWT
VEOG	8 (9)	5 (4)	3 (3)	7 (7)	4 (6)
HEOG	10 (10)	5 (8)	-5 (1)	1 (9)	-8 (1)
EOG	6 (8)	2 (2)	1 (1)	5 (7)	4 (6)
EMG_{rail1}	-	7 (10)	2 (5)	6 (10)	-1 (2)
EMG_{rail2}	-	10 (10)	1 (5)	5 (10)	-3 (1)
EMG_{rail3}	-	10 (13)	1 (8)	6 (10)	0 (2)
$\mathbf{EMG}_{rail}$	-	9 (13)	5 (9)	8 (10)	5 (8)
EMG_{noise1}	-	7 (10)	3 (5)	6 (10)	0 (2)
EMG_{noise2}	-	11 (10)	3 (7)	7 (10)	2 (4)
EMG_{noise3}	-	6 (10)	-2 (1)	2 (7)	-8 (-1)
$\mathbf{EMG}_{noise}$	-	8 (10)	4 (8)	7 (10)	2 (6)
EOGnEMG	-	2 (4)	2 (3)	5 (7)	4 (5)

TABLE II
COMPARISON BETWEEN THE DIFFERENCE COMBINATION OF ARTIFACT REMOVAL METHOD FOR EYES-OPENED AND EYES-CLOSED CONDITION (EYES OPENED IN BRACKET)

Artifacts	SOBI vs ICA	SWT vs DWT
VEOG	-1.5 (-3)	2.5 (1)
HEOG	3.5 (-0.5)	9.5 (7.5)
EOG	-3 (-5)	1 (1)
EMG_{rail1}	2 (1.5)	6 (6.5)
EMG_{rail2}	4.5 (2)	8.5 (7)
EMG_{rail3}	2.5 (4.5)	7.5 (6.5)
$\mathbf{EMG}_{rail}$	0.5 (2)	3.5 (3)
EMG_{noise1}	2 (1.5)	5 (6.5)
EMG_{noise2}	2.5 (1.5)	6.5 (4.5)
EMG_{noise3}	5 (2.5)	9 (8.5)
$\mathbf{EMG}_{noise}$	1.5 (1)	4.5 (3)
EOGnEMG	-2.5 (-2.5)	0.5 (1.5)

of BSS or wavelet algorithm would contribute more to the increase in performance for artifact removal. Table II shows the comparison of using SOBI instead of ICA while fixing the wavelet method used as well as SWT instead of DWT while fixing the BSS used. It can be seen that when ICA is replaced with SOBI, an increase of about 2 dB in performance is only seen in the EMG artifacts. However, the performance seemed to deteriorate for EOG artifacts. When SWT is compared against DWT, it can be seen that the increase in performance is about 6 dB for the EMG artifacts. Although the EOG artifacts also indicate an increase in performance, the case of VEOG and EOG increased the performance by only 1 dB. This may be rather small and should be considered as negligible. The HEOG artifacts removal is increased by about 8 dB. It is interesting to note that the increase in performance is slightly more (about 0.5 dB) for eyes-closed condition as compared to eyes-opened condition. This is rather obvious as the performance of eyes-closed condition is slightly inferior to the eyes-opened condition (refer Table I) and thus has more room for improvement.

B. Relative Root Mean Squared Error

The analysis using RRMSE on the different frequency band would enhance our understanding on the performance of the methods. Fig. 5 shows the RRMSE of the EEG component after artifact removal for EOGnEMG artifact. Fig. 5(a)–(d) refers to the segment of data that originally contained artifacts while Fig. 5(e)–(h) refers to the segment of data that was originally clean. It is assumed that the performance of the algorithm is acceptable if the RRMSE <0.1 (shown by a broken line).

Based on Fig. 5(a), all the methods seemed to have removed the δ frequency band EEG signals along with the artifacts. One possible reason is that the HEOG affects the whole segment of data. Thus, removal of HEOG also removes the EEG at the same frequency component. It should be noted that as the SNR increases, the EEG in the δ frequency band produce acceptable results for SOBI-SWT as well as SOBI-DWT. A possible explanation is that as the SNR increased, these algorithms do not remove the EOG component as it is too weak to be detected [refer Fig. 4(a)].

The θ frequency band for all the methods produced unacceptable results. This can be seen in Fig. 5(b). For the α frequency band, the performance of SOBI-SWT is slightly better than the other algorithm [refer Fig. 5(c)]. The other three methods are hovering around the acceptable region. In the β frequency band, we have SOBI-SWT outperforming the rest yet again, as seen in Fig. 5(d). However, it should be noted that the performance of ICA-SWT is only slightly inferior to SOBI-SWT. It seems that the combinations that used DWT performed relatively poor in the β frequency band.

For the segment of data that was originally uncontaminated from artifacts, SOBI-SWT performs better or at least as good as all the other methods for all the frequency bands as shown in Fig. 5(e)–(h). For the δ frequency band, SOBI-SWT produces acceptable results for all the SNR while ICA-DWT is slightly below the acceptable threshold. The other two methods have very similar performances and produce results that are slightly above the acceptable threshold. All the methods produce results that are below the acceptable threshold for the θ frequency band. This weakness probably occurs due to the sporadic nature of the θ rhythm. Thus, the wavelet-denoising method may have considered the sudden increase of θ rhythm to be an artifact and thus unintentionally removed it. As for the α and β frequency bands, all the methods produced acceptable results. The combination that used SWT removed less α frequency components [refer Fig. 5(g)]. In the β frequency band, SOBI-SWT is clearly superior to the other methods.

V. EXPERIMENTAL STUDIES ON EXTRACTION OF THE μ RHYTHM

In this section, two experiments are carried out to verify the effectiveness of the two-stage approach as compared with the direct application of the SOBI method in extracting the μ rhythm. The first experiment used simulated data where the effects of different SNR to the five different algorithms are compared. In the second experiment, the actual EEG data from ten subjects are used. The algorithm used in this study are

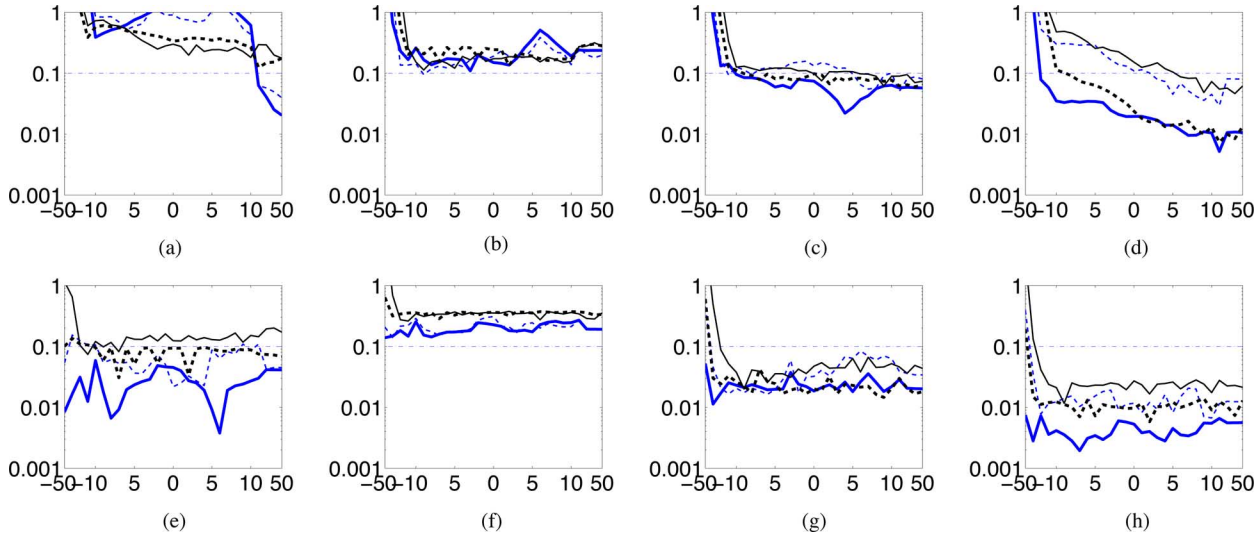

Fig. 5. Comparison between the performance of SOBI-SWT (thick continuous line), SOBI-DWT (thin broken line), ICA-SWT (thick broken line), and ICA-DWT (thin continuous line) for different frequency bands for all the artifacts. The y-axis indicates the RRMSE while the x-axis is the SNR of the artifact mixture in dB. (a) δ artifacts. (b) θ artifacts. (c) α artifacts. (d) β artifacts. (e) δ signal. (f) θ signal. (g) α signal. (h) β signal.

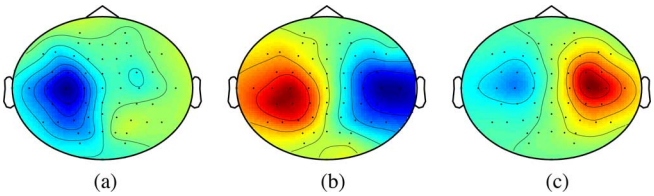

Fig. 6. Three different topographical plots that exist for μ rhythm component. (a) LEFT. (b) BOTH. (c) RIGHT.

SOBI, SOBI-SWT-SOBI, SOBI-DWT-SOBI, ICA-SWT-SOBI, and ICA-DWT-SOBI.

A. Experiment Using Simulated EEG Data

As stated in Section III, the simulated EEG data are obtained by filtering the EEG data from three subjects. Typically, there are three types of topographical plot that exist as shown in Fig. 6 that indicates the μ rhythm component for the hand movement. In order to classify them, certain naming conventions are used. LEFT would indicate the presence of the μ rhythm on the left hemisphere. This can be seen by the darker colors at around the left motor cortex area as shown in Fig. 6(a). Likewise, the same is referred for BOTH and RIGHT.

Table III shows the ability of the five different methods in extracting the μ rhythm. For clarity, the SNR is grouped into low SNR (-50 to -10 dB), moderate SNR (-9 to 9 dB), and high SNR (10 to 50 dB). It should be noted that for low SNR, the total number of cases are 15 (5 different SNR $\times$ 3 subjects) while the moderate SNR have a total of 57 cases (19 different SNR $\times$ 3 subjects) and high SNR also has a total of 15 cases (5 different SNR $\times$ 3 subjects). The values 0, 1, 2, and 3 on the top of Table III corresponds to the number of μ rhythm components that can be found. Since the number of cases is different for all the different SNR groups, the values shown in the table are the percentage of cases that were able to find the corresponding number of μ rhythm components.

1) Low SNR: When SOBI is directly applied on to the original data without artifact removal, it encounters difficulty in extracting the μ rhythm. For example, it can be seen from Table III that when only SOBI is used, 47% of the cases could not extract even a single μ rhythm component. By applying the two-stage methods such as SOBI-SWT-SOBI and SOBI-DWT-SOBI, every case had at least one μ rhythm component. It can be seen that SOBI-SWT-SOBI outperforms all other combinations. One possible reason is that the ICA-combined algorithms may have removed slightly more EEG signals.

2) Moderate SNR: As the SNR increases from the low SNR group to the moderate SNR group, all the five methods would extract at least one μ rhythm component. However, the direct application of SOBI has only 14% of the cases where all the three μ rhythm components are extracted. Even in this group, the proposed method of SOBI-SWT-SOBI again produced the best performance by having 63% of the cases where all the three μ rhythm components are extracted.

3) High SNR: All the five methods could extract all the three μ rhythm components when the SNR is high. This is probably because the artifacts are so weak that they can be considered negligible.

Generally, we can see that the two-stage methods could extract μ rhythm components more efficiently than SOBI for low and moderate SNR. As for the high SNR, the performance of all the algorithms are comparable. Among the four types of artifact removal methods for the two-stage method, SOBI-SWT-SOBI has the best performance at extracting the μ rhythm components.

B. Experiment Using Actual EEG Data

The five different methods applied on to the simulated data are now applied on to the actual EEG data of the ten subjects.

TABLE III
PERCENTAGE OF THE INDEPENDENT COMPONENT THAT INDICATES THE EXISTENCE OF THE TOPOGRAPHICAL PLOT

Methods	SOBI				SOBI-SWT-SOBI				SOBI-DWT-SOBI				ICA-SWT-SOBI				ICA-DWT-SOBI			
μ components	0	1	2	3	0	1	2	3	0	1	2	3	0	1	2	3	0	1	2	3
Low	47	27	27	0	0	7	47	47	0	40	53	7	13	33	40	13	20	20	53	7
Moderate	0	26	60	14	0	4	33	63	0	4	44	53	0	7	44	49	0	11	54	35
High	0	0	0	100	0	0	0	100	0	0	0	100	0	0	0	100	0	0	0	100

TABLE IV
INDEPENDENT COMPONENT INDICATING EXISTENCE OF THE TOPOGRAPHICAL PLOT FOR EYES CLOSED

Subjects	SOBI			SOBI-SWT-SOBI			SOBI-DWT-SOBI			ICA-SWT-SOBI			ICA-DWT-SOBI		
	Left	Both	Right	Left	Both	Right	Left	Both	Right	Left	Both	Right	Left	Both	Right
S1	-	-	7	8	5	12	7	5	15	14	-	7	6	-	16
S2	-	-	-	-	13	-	55	-	-	-	14	-	-	-	-
S3	-	37	-	50	39	19	40	29	34	46	37	24	54	30	-
S4	-	40	-	-	40	-	-	51	-	-	34	-	-	52	-
S5	-	20	-	21	-	6	9	-	18	14	-	7	8	5	-
S6	42	-	31	14	-	8	53	-	8	45	-	8	19	-	8
S7	12	-	53	13	6	11	22	19	-	4	22	-	-	3	-
S8	17	8	49	18	17	9	-	7	18	-	7	18	18	9	-
S9	51	-	39	12	-	33	20	-	44	15	-	20	42	-	6
S10	-	36	-	-	35	-	-	15	-	-	34	-	-	-	19

TABLE V
INDEPENDENT COMPONENT INDICATING EXISTENCE OF THE TOPOGRAPHICAL PLOT FOR EYES OPENED

Subjects	SOBI			SOBI-SWT-SOBI			SOBI-DWT-SOBI			ICA-SWT-SOBI			ICA-DWT-SOBI		
	Left	Both	Right	Left	Both	Right	Left	Both	Right	Left	Both	Right	Left	Both	Right
S1	28	-	38	21	5	24	33	24	16	7	-	23	7	-	23
S2	-	-	47	49	-	47	49	-	50	34	-	51	55	-	45
S3	25	-	34	24	36	35	34	25	30	26	30	32	27	28	32
S4	-	38	-	34	-	42	34	-	37	-	-	39	-	-	32
S5	-	28	-	21	48	-	16	23	-	-	20	-	-	29	-
S6	-	48	-	28	-	37	10	-	39	10	-	27	42	-	10
S7	33	27	-	49	24	47	14	-	5	17	-	26	31	-	15
S8	5	7	22	8	11	18	8	5	15	44	49	22	21	-	22
S9	33	-	32	-	17	41	41	9	36	-	17	-	-	17	33
S10	25	-	-	-	47	-	-	18	-	-	20	-	-	26	-

The data considered here are of the eyes-closed as well as eyes-opened conditions. The results for all the ten subjects using the five different methods for the eyes-closed condition (refer Table IV) as well as eyes-opened condition (refer Table V) are shown. The values in these tables indicate the SOBI component number where the corresponding μ rhythm was found.

For example, when SOBI is directly applied on to the raw EEG data in the eyes-closed condition (refer Table IV), the 7th SOBI component indicates the presence of the RIGHT μ rhythm for S1. It can be seen that the proposed method, SOBI-SWT-SOBI showed the presence of all the three μ rhythm components at the 8th, 5th, and 12th SOBI component for the RIGHT, BOTH, and LEFT, respectively.

1) Eyes-Closed Condition: When the SOBI-SWT-SOBI method is compared with the direct application of the SOBI method, it is found that the performance of the μ rhythm component extraction has improved. Five subjects have shown more μ rhythm components and three other subjects have more dominant μ rhythm components while the remaining two subjects do not indicate much improvement in performance (S4 and S10). The ability to extract the μ rhythm for SOBI-DWT-SOBI is rather similar to ICA-SWT-SOBI. Both methods showed more μ rhythm components in three subjects and one subject indicated less μ rhythm components (S8) as compared with the direct application of SOBI. However, the ICA-DWT-SOBI produced mixed results when compared with SOBI. One possible reason for this inconsistent result is that although the two-stage method successfully removed artifacts, the ICA-DWT has shown to remove relatively more EEG components as compared to the other artifact removal methods. Thus, SOBI-SWT-SOBI, which removed the least EEG components as demonstrated in Section IV, would either improve or at least maintain the performance as compared with the direct application of SOBI.

2) Eyes-Opened Condition: When Table V is compared with Table IV, it can be seen that for the eyes-opened condition more μ rhythm components could be extracted. This is to be expected as the eyes-opened condition suppressed the visual α rhythm that could obscure the extraction of the μ rhythm component. We can see that both the application of SOBI-SWT-SOBI and SOBI-DWT-SOBI have improved the extraction of the μ rhythm of seven subjects. The ICA-SWT-SOBI and ICA-DWT-SOBI on the other hand only manage to improve the extraction of the μ rhythm component from three subjects. However, one of

the subjects showed a weaker performance as compared to the direct application of SOBI.

To summarize the results from the actual EEG data, we found that the two-stage method using SOBI-SWT-SOBI would improve the extraction of the μ rhythm component as compared with the other four methods. It has been stated that the direct application of SOBI would have difficulty in the extraction of the μ rhythm component in the presence of EMG artifacts [46]. Based on the study of artifact removal, we have found that the SOBI-SWT method is the most effective method to be applied for the first stage in this two-stage approach to extract the μ rhythm.

VI. Conclusion

In this paper, we demonstrated a two-stage method to extract μ rhythm components in the presence of EOG and EMG artifacts. The first stage is used to remove artifacts while the second stage is used to extract the μ rhythm components. Our proposed method of SOBI-SWT is compared with SOBI-DWT, ICA-SWT, ICA-DWT, and regression method to remove the artifacts. It was found that the proposed algorithm based on SOBI-SWT is most effective in removing EMG. As for the EOG artifacts, the regression method performs best. As for the second stage, a standard SOBI method is then applied on to each of the processed signal of the first stage to extract the μ rhythm components.

The direct application of SOBI is compared with each of the four two-stage methods. Two types of experiments are carried out to determine the effectiveness of the two-stage methods. In the first experiment, the results from the simulated data indicate that the two-stage methods outperformed the direct application of SOBI for low and moderate SNR in extracting the μ rhythm. However, at high SNR the performance of all the algorithms are similar. It should be noted that for practical considerations, the interest is on producing better performance for low and moderate SNR. The proposed SOBI-SWT-SOBI method outperforms the other two-stage methods. In the second experiment, these five methods are then tested on to actual EEG data from ten subjects. Generally, it can be seen that SOBI-SWT-SOBI outperforms the other methods in extracting the μ rhythm component for most of the subjects.

The usage of the regression method would be an effective way of removing EOG artifacts without removing the δ and θ frequencies. In order to improve the proposed SOBI-SWT algorithm, more advanced artifact detection methods, such as kurtosis [48], probability density function [26], and entropy [49], could be incorporated.

Acknowledgment

The authors would like to thank the reviewers for their invaluable comments and suggestions.

References

[1] A. Stančák, A. Riml, and G. Pfurtscheller, "The effects of external load on movement-related changes of the sensorimotor EEG rhythms," *EEG Clin. Neurophysiol.*, vol. 102, no. 6, pp. 495–504, 1997.

[2] N. Erbil and P. Ungan, "Changes in the alpha and beta amplitudes of the central EEG during the onset, continuation, and offset of long-duration repetitive hand movements," *Brain Res.*, vol. 1169, pp. 44–56, 2007.

[3] R. de Jong, T. Gladwin, and B. 't Hart, "Movement-related EEG indices of preparation in task switching and motor control," *Brain Res.*, vol. 1105, no. 1, pp. 73–82, 2006.

[4] G. Pfurtscheller and C. Neuper, "Motor imagery activates primary sensorimotor area in humans," *Neurosci. Lett.*, vol. 239, no. 2/3, pp. 65–68, 1997.

[5] G. Pfurtscheller, C. Neuper, C. Andrew, and G. Edlinger, "Foot and hand area mu rhythms," *Int. J. Psychophysiol.*, vol. 26, no. 1–3, pp. 121–135, 1997.

[6] E. Labyt, W. Szurhaj, J. Bourriez, F. Cassim, L. Defebvre, A. Destée, and P. Derambure, "Influence of aging on cortical activity associated with a visuo-motor task," *Neurobiol. Aging*, vol. 25, no. 6, pp. 817–827, 2004.

[7] G. Cheron, A. Leroy, C. De Saedeleer, A. Bengoetxea, M. Lipshits, A. Cebolla, L. Servais, B. Dan, A. Berthoz, and J. McIntyre, "Effect of gravity on human spontaneous 10-Hz electroencephalographic oscillations during the arrest reaction," *Brain Res.*, vol. 1121, no. 1, pp. 104–116, 2006.

[8] T. Stroganova, G. Nygren, M. Tsetlin, I. Posikera, C. Gillberg, M. Elam, and E. Orekhova, "Abnormal EEG lateralization in boys with autism," *Clin. Neurophysiol.*, vol. 118, no. 8, pp. 1842–1854, 2007.

[9] N. Virji-Babul, A. Moiseev, T. Cheung, D. Weeks, D. Cheyne, and U. Ribary, "Changes in mu rhythm during action observation and execution in adults with Down syndrome: Implications for action representation," *Neurosci. Lett.*, vol. 436, pp. 177–180, 2008.

[10] J. Diez, G. Pfurtscheller, F. Reisecker, B. Ortmayr, and K. Zalaudek, "Event-related desynchronization and synchronization in idiopathic Parkinson's disease," *EEG Clin. Neurophysiol.*, vol. 103, no. 1, pp. 155–155, 1997.

[11] J. A. Pineda, D. Brang, E. Hecht, L. Edwards, S. Carey, M. Bacon, C. Futagaki, D. Suk, J. Tom, C. Birnbaum, and A. Rork, "Positive behavioral and electrophysiological changes following neurofeedback training in children with autism," *Res. Autism Spect. Disorders*, vol. 2, pp. 557–581, 2008.

[12] D. Krusienski, G. Schalk, D. McFarland, and J. Wolpaw, "A μ-rhythm matched filter for continuous control of a brain–computer interface," *IEEE Trans. Biomed. Eng.*, vol. 54, no. 2, pp. 273–280, Feb. 2007.

[13] G. Pfurtscheller, C. Brunner, A. Schlögl, and F. Lopes da Silva, "Mu rhythm (de) synchronization and EEG single-trial classification of different motor imagery tasks," *Neuroimage*, vol. 31, no. 1, pp. 153–159, 2006.

[14] E. Niedermeyer, "The normal eeg of the waking adult," in *Electroencephalography: Basic Principles, Clinical Applications, and Related Fields*, 5th ed. Philadelphia, PA: Lippincott Williams & Wilkins, 2005, pp. 167–192.

[15] G. Pfurtscheller and A. Aranibar, "Evaluation of event-related desynchronization (ERD) preceding and following voluntary self-paced movement," *EEG Clin. Neurophysiol.*, vol. 46, no. 2, pp. 138–146, 1979.

[16] C. Ochoa and J. Polich, "P300 and blink instructions," *Clin. Neurophysiol.*, vol. 111, no. 1, pp. 93–98, 2000.

[17] D. Blum, "Computer-based electroencephalography: Technical basics, basis for new applications, and potential pitfalls," *EEG Clin. Neurophysiol.*, vol. 106, no. 2, pp. 118–126, 1998.

[18] S. Selvan and R. Srinivasan, "Removal of ocular artifacts from EEG using an efficient neural network based adaptive filtering technique," *IEEE Signal Process Lett.*, vol. 6, no. 12, pp. 330–332, Dec. 1999.

[19] C. Melissant, A. Ypma, E. Frietman, and C. Stam, "A method for detection of Alzheimer's disease using ICA-enhanced EEG measurements," *AI Med.*, vol. 33, no. 3, pp. 209–222, 2005.

[20] J. Jiang, C. Chao, M. Chiu, R. Lee, C. Tseng, and R. Lin, "An automatic analysis method for detecting and eliminating ECG artifacts in EEG," *Comp. Biol. Med.*, vol. 37, no. 11, pp. 1660–1671, 2007.

[21] T. Zikov, S. Bibian, G. Dumont, M. Huzmezan, and C. Ries, "A wavelet based de noising technique for ocular artifact correction of the electroencephalogram," in *Proc. Second Joint EMBS/BMES Conf.*, 2002, vol. 1, pp. 98–105.

[22] J. Kierkels, G. van Boxtel, and L. Vogten, "A model-based objective evaluation of eye movement correction in EEG recordings," *IEEE Trans. Biomed. Eng.*, vol. 53, no. 2, pp. 246–253, Feb. 2006.

[23] A. Kachenoura, H. Gauvrit, and L. Senhadji, "Extraction and separation of eyes movements and the muscular tonus from a restricted number of electrodes using the independent component analysis," in *Proc. 25th Annu. Int. Conf. IEEE EMBS*, 2003, vol. 3, pp. 2359–2362.

[24] P. LeVan, E. Urrestarazu, and J. Gotman, "A system for automatic artifact removal in ictal scalp EEG based on independent component analysis and Bayesian classification," *Clin. Neurophysiol.*, vol. 117, no. 4, pp. 912–927, 2006.
[25] W. Zhou, "Removal of ECG artifacts from EEG using ICA," in *Proc. Second Joint EMBS/BMES Conf.*, Houston, TX, Oct. 2002, pp. 206–207.
[26] L. Shoker, S. Sanei, and J. Chambers, "Artifact removal from electroencephalograms using a hybrid BSS–SVM algorithm," *IEEE Signal Process. Lett.*, vol. 12, no. 10, pp. 721–724, Oct. 2005.
[27] G. Gómez-Herrero, W. De Clercq, H. Anwar, O. Kara, K. Egiazarian, S. Van Huffel, and W. Van Paesschen, "Automatic removal of ocular artifacts in the eeg without a reference eog channel," in *Proc. 7th Nordic Signal Process. Symp. (NORSIG)*, 2006, pp. 130–133.
[28] S. Romero, M. Mañanas, and M. Barbanoj, "A comparative study of automatic techniques for ocular artifact reduction in spontaneous EEG signals based on clinical target variables: A simulation case," *Comp. Biol. Med.*, vol. 38, no. 3, pp. 348–360, 2008.
[29] N. Castellanos and V. Makarov, "Recovering EEG brain signals: Artifact suppression with wavelet enhanced independent component analysis," *J. Neurosci. Methods*, vol. 158, no. 2, pp. 300–312, 2006.
[30] G. Inuso, F. La Foresta, N. Mammone, and F. Morabito, "Wavelet-ICA methodology for efficient artifact removal from electroencephalographic recordings," in *Proc. Int. Joint Conf. Neural Netw. (IJCNN 2007)*, pp. 1524–1529.
[31] S. Makeig, A. Bell, T. Jung, and T. Sejnowski, "Independent component analysis of electroencephalographic data," in *Proc. Adv. Neural Inf. Proc. Syst.*, 1996, pp. 145–151.
[32] R. Brychta, R. Shiavi, D. Robertson, and A. Diedrich, "Spike detection in human muscle sympathetic nerve activity using the kurtosis of stationary wavelet transform coefficients," *J. Neurosci. Methods*, vol. 160, no. 2, pp. 359–367, 2007.
[33] R. Brychta, S. Tuntrakool, M. Appalsamy, N. Keller, D. Robertson, R. Shiavi, and A. Diedrich, "Wavelet methods for spike detection in mouse renal sympathetic nerve activity," *IEEE Trans. Biomed. Eng.*, vol. 54, no. 1, pp. 82–93, Jan. 2007.
[34] S. Boudet, L. Peyrodie, P. Gallois, and C. Vasseur, "Filtering by optimal projection and application to automatic artifact removal from EEG," *Signal Process.*, vol. 87, no. 8, pp. 1978–1992, 2007.
[35] B. Noureddin, P. Lawrence, and G. Birch, "Time–frequency analysis of eye blinks and saccades in EOG for EEG artifact removal," in *Proc. 3rd Int. IEEE/EMBS Conf. Neural Eng. (CNE 2007)*, pp. 564–567.
[36] I. Goncharova, D. McFarland, T. Vaughan, and J. Wolpaw, "EMG contamination of EEG: Spectral and topographical characteristics," *Clin. Neurophysiol.*, vol. 114, no. 9, pp. 1580–1593, 2003.
[37] G. Wallstrom, R. Kass, A. Miller, J. Cohn, and N. Fox, "Automatic correction of ocular artifacts in the EEG: A comparison of regression-based and component-based methods," *Int. J. Psychophysiol.*, vol. 53, no. 2, pp. 105–119, 2004.
[38] B. Azzerboni, M. Carpentieri, F. La Foresta, and F. Morabito, "Neural-ICA and wavelet transform for artifacts removal in surface EMG," in *Proc. IEEE Int. Joint Conf. Neural Netw.*, 2004, vol. 4, pp. 3223–3228.
[39] G. Pfurtscheller, C. Neuper, A. Schlogl, and K. Lugger, "Separability of EEG signals recorded during right and left motorimagery using adaptive autoregressive parameters," *IEEE Trans. Rehabil. Eng.*, vol. 6, no. 3, pp. 316–325, Sep. 1998.
[40] C. Jutten and A. Taleb, "Source separation: From dusk till dawn," in *Proc. 2nd Int. Workshop ICA BSS (ICA 2000)*, pp. 15–26.
[41] A. Hyvarinen, J. Karhunen, and E. Oja, *Independent Component Analysis*. New York: Wiley, 2001.
[42] A. Belouchrani, K. Abed-Meraim, J. Cardoso, and E. Moulines, "A blind source separation technique using second-order statistics," *IEEE Trans. Signal Process.*, vol. 45, no. 2, pp. 434–444, Feb. 1997.
[43] A. Belouchrani and A. Cichocki, "Robust whitening procedure in blind source separation context," *Electron. Lett.*, vol. 36, no. 24, pp. 2050–2053, 2000.
[44] A. Cichocki and S. Amari, *Adaptive Blind Signal and Image Processing: Learning Algorithms and Applications*. New York: Wiley, 2002.
[45] W. Zhou and J. Gotman, "Removal of EMG and ECG artifacts from EEG based on wavelet transform and ICA," in *Proc. Conf. 26th Annu. Int. Conf. EMBS 2004*, vol. 1, pp. 392–395.
[46] J. Onton and S. Makeig. "Information-based modeling of event-related brain dynamics," *Prog. Brain Res.,* vol. 159, pp. 99–120, 2006.
[47] I. Dimatteo, C. Genovese, and R. Kass, "Bayesian curve-fitting with free-knot splines," *Biometrika*, vol. 88, no. 4, pp. 1055–1071, 2001.
[48] A. Delorme, T. Sejnowski, and S. Makeig, "Enhanced detection of artifacts in EEG data using higher-order statistics and independent component analysis," *Neuroimage*, vol. 34, no. 4, pp. 1443–1449, 2007.
[49] G. Inuso, F. la Foresta, N. Mammone, and F. Morabito, "Brain activity investigation by EEG processing: Wavelet analysis, Kurtosis and Renyi's entropy for artifact detection," in *Proc. Int. Conf. Inf. Acquisition (ICIA 2007)*, pp. 195–200.

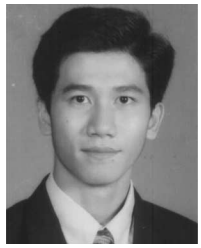

Siew-Cheok Ng received the B.Eng. degree in mechanical engineering and the M.S. degree in engineering science in 2000 and 2003, respectively, from the University of Malaya, Kuala Lumpur, Malaysia, where he is currently working toward the Ph.D. degree at the Department of Biomedical Engineering.

His current research interests include biomedical signal processing, pattern recognition, and brain–computer interface technology.

Paramesran Raveendran (S'94-M'95–SM'03) received the B.Sc. and M.Sc. degrees in electrical engineering from South Dakota State University, Brookings, in 1984 and 1985, respectively, and the Dr. Eng degree from the University of Tokushima, Tokushima, Japan, in 1994.

He was a System Designer with Daktronics. In 1986, he joined the Department of Electrical Engineering, University of Malaya, Kuala Lumpur, Malaysia, where he is currently a Professor. His research interests include image analysis, image reconstruction, brain–computer interface technology, and biomedical signal analysis.